A One-Dimensional Fluid Model for an Acetylene RF Discharge: A Study of the Plasma Chemistry

Dieter Herrebout, Annemie Bogaerts, Renaat Gijbels, Willem Jan Goedheer, and Annick Vanhulsel

***Abstract*—A one-dimensional (1-D) fluid model is developed for an RF acetylene discharge. In total, 24 species (neutrals, radicals, electrons, and ions) are considered. For every species, a mass balance equation is solved. Further, the electron energy equation and the Poisson equation are also considered. Reactions taken into account include 19 electron–neutral, one ion–neutral, and 17 neutral–neutral reactions. The reaction rate coefficients of the ion–neutral and neutral–neutral reactions are taken from literature. The rate coefficients of the electron-neutral reactions depend strongly on the average electron energy, and are, therefore, obtained from a simplified Boltzmann equation. The 1-D fluid model yields, among others, information about the densities of the different species in the plasma. The most important neutral species in an acetylene plasma are C_2H_2 and H_2. Further, the radicals C_4H_2, C_6H_2, and C_8H_2 (to a minor extent) are also present at high densities. These higher order carbon radicals are mainly formed in neutral–neutral reactions with C_2H. Other radical species present at high densities are H, C_2H_3, CH_2, and C_xH (with x equal to 2, 4, and 6). The most important ionic species are found to be $C_4H_2^+$, $C_2H_2^+$, and $C_6H_2^+$. Finally, a comparison is made between an acetylene and a methane plasma.**

***Index Terms*—Acetylene discharges, plasma modeling.**

I. INTRODUCTION

DIAMOND-LIKE carbon (DLC) layers are frequently deposited on a variety of substrates as a protective layer. These amorphous carbon layers (a-C:H) are widely used because they combine some interesting characteristics: high hardness, very low friction coefficient, chemical inertness, and infrared transparancy. Normally, plasma assisted chemical vapor deposition (PACVD) is used for the deposition of these DLC layers, utilizing hydrocarbon gases such as methane [1]–[4] and acetylene [5]–[12]. For the use of acetylene as input gas, different plasma types are reported in literature: a capacitively coupled RF (13.56 MHz) discharge [5], [6], a microwave discharge [7], [8], or an expanding arc plasma [9]–[12]. An overview of the different kinds of methane plasmas is given in [1].

In this paper, a one-dimensional (1-D) fluid model will be used to study capacitively coupled RF acetylene discharges. Whereas, in the study of Doyle [5], the work is emphasized on the production and gas depletion in acetylene discharges (i.e., calculation of production rates of C_4H_2 and C_6H_2, and comparison with experimental results), our theoretical model considers the role of charged species, in combination with the neutral–neutral chemistry. In [6], a detailed experimental study of capacitively coupled RF acetylene plasmas is done by Vasile *et al.* where also the main neutral–neutral and ion–neutral reactions are discussed.

The acetylene plasma chemistry model itself (species and reactions) is described in detail in Section II, whereas the results will be presented in Section III. Finally, the conclusions are given in Section IV.

II. DESCRIPTION OF THE 1-D FLUID MODEL

The fluid model used for the study of C_2H_2 plasmas was originally developed for the modeling of silane plasmas [13]–[15]. Later on, it was also used for the study of methane plasmas [1]. The fluid model itself contains the following equations: for every species, a mass balance equation is considered. Further, the Poisson equation and the electron energy equation are taken into account. From the Poisson equation, the electric field is obtained ($E = -\nabla V$). Since the ions cannot follow the actual RF field, an effective field is used [13]. The combination of the electron energy equation and the electron density balance equation gives us the average electron energy, as a function of space (between the electrodes) and time in the RF cycle. This average electron energy is used to obtain the corresponding electron mobility and diffusion coefficients, and the reaction rate coefficients for every electron-neutral reaction. These coefficients are found by interpolation in lookup tables generated with a simplified Boltzmann solver [1], [13]–[15]. Indeed, for a given density and composition of the background gas the electron energy distribution function (EEDF) is computed for a range of values of the electric field. This yields combinations of average electron energies and corresponding coefficients, that are stored in the look-up tables. The transport coefficients of the other plasma species (neutrals, radicals, and ions) are calculated from the equations described in detail in [1], [13]–[15].

The power going into the plasma is transferred to the charged species by Ohmic heating. In the fluid model, the value of V_{rf} (i.e., the amplitude of the potential applied at the powered electrode) is adapted iteratively to fit the input value of the power. No bias voltage (V_{dc}) can be applied because of the limitations of the 1-D fluid model. For more information, we refer to [13] and [14].

A Sharfetter–Gummel exponential scheme is used for the finite volume discretization of all the equations in the fluid model.

Manuscript received December 11, 2002; revised February 19, 2003. This work was supported by the Vlaamse Instelling voor Technologisch onderzoek (VITO), by the Federal Services for Scientific, by the Technical and Cultural Affairs (DWTC/SSTC) of the Prime Minister's Office through IUAP V, and by the Flemish Fund for Scientific Research (FWO).

D. Herrebout, A. Bogaerts, and R. Gijbels are with the Department of Chemistry, University of Antwerp, 2610 Wilrijk, Belgium (e-mail: bogaerts@uia.ua.ac.be).

W. J. Goedheer is with the FOM-Institute for Plasma Physics RIJNHUIZEN, 3430 BE Nieuwegein, The Netherlands.

A. Vanhulsel is with the Vlaamse Instelling voor Technologisch Onderzoek (VITO), 2400 Mol, Belgium.

Digital Object Identifier 10.1109/TPS.2003.815249

TABLE I
DIFFERENT SPECIES TAKEN INTO ACCOUNT IN THE C_2H_2 PLASMA MODEL, BESIDE ELECTRONS

Neutrals	Radicals				Ions	
C_2H_2	C_4H_2	C_6H_2	H	C_8H	$C_2H_2^+$	C_2H^+
H_2	CH	CH_2	C_2H		C_2^+	CH^+
	C_2H_3	C_4H_3	C_6H_3		C^+	H_2^+
	C_4H	C_6H	C_8H_2		$C_4H_2^+$	$C_6H_2^+$

TABLE II
ELECTRON–NEUTRAL REACTIONS TAKEN INTO ACCOUNT IN THE MODEL, AS WELL AS THE REFERENCES FROM WHERE THE CROSS SECTIONS ARE TAKEN

Reaction	Chemical reaction	Ref.
	C_2H_2	
vibr. exc.	$e^- + C_2H_2 \rightarrow C_2H_2^* + e^-$ (3)	16
ionisation	$e^- + C_2H_2 \rightarrow C_2H_2^+ + 2\,e^-$	16
ionisation	$e^- + C_2H_2 \rightarrow C_2H^+ + H + 2\,e^-$	16
ionisation	$e^- + C_2H_2 \rightarrow C_2^+ + H_2 + 2\,e^-$	16
ionisation	$e^- + C_2H_2 \rightarrow CH^+ + CH + 2\,e^-$	16
ionisation	$e^- + C_2H_2 \rightarrow C^+ + CH_2 + 2\,e^-$	16
dissociation	$e^- + C_2H_2 \rightarrow C_2H + H + e^-$	17
	H_2	
vibr. exc.	$e^- + H_2 \rightarrow H_2^* + e^-$ (3)	18
dissociation	$e^- + H_2 \rightarrow 2\,H + e^-$	19
ionisation	$e^- + H_2 \rightarrow H_2^+ + 2\,e^-$	20
	C_4H_2	
dissociation	$e^- + C_4H_2 \rightarrow C_4H + H + e^-$	*
ionisation	$e^- + C_4H_2 \rightarrow C_4H_2^+ + 2\,e^-$	*
	C_6H_2	
dissociation	$e^- + C_6H_2 \rightarrow C_6H + H + e^-$	*
ionisation	$e^- + C_6H_2 \rightarrow C_6H_2^+ + 2\,e^-$	*
	C_8H_2	
dissociation	$e^- + C_8H_2 \rightarrow C_8H + H + e^-$	*

The number of different vibrational excitation (vibr. exc.) reactions is given between brackets.

(*): reactions for which no cross sections data were found in literature, and hence estimations had to be made.

The distance between the two electrodes (3 cm) is divided in 64 cells. Further, a fully implicit method is used to solve these equations in a self-consistent way. In order to avoid numerical instabilities, the time step in the RF cycle (13.56 MHz) is set to $9.2 \cdot 10^{-10}$ s (i.e., the RF cycle is divided in 80 time steps). The input parameters in the fluid model are: the power; the pressure; and the reactor geometry. The convergence criterion in the fluid model is set to 10^{-6} (i.e., the error which is allowed between the plasma characteristics (species densities, potential,...) calculated in two subsequent RF cycles). Since the fluid model requires data from the Boltzmann model and vice versa (because of the changes in the gas composition), both models are iterated, until the differences in background densities (i.e., the species involved in the electron-neutral reactions, and present at high density) calculated in two successive fluid runs reach an value of less than 10^{-4}.

The species considered in the model for acetylene, beside the electrons, are given in Table I. The main neutral species are C_2H_2 and H_2. Thirteen radical species are included, of which the carbon rich species C_xH_y (with $x > y$) are present in large amounts [5], [6]. Further, eight ionic species are considered. As an approximation, the ionic species $C_2H_2^+$ and $C_2H_3^+$ are considered as one species, namely $C_2H_2^+$. In the same way, $C_4H_2^+$ and $C_6H_2^+$ represent, respectively, the ions $C_4H_2^+$, $C_4H_3^+$, and $C_6H_2^+$ and $C_6H_3^+$. In Table II, the 19 electron–neutral reactions taken into account in the model are presented. These electron–neutral reactions can be divided in three categories: vibrational excitation, dissociation, and ionization reactions. Electron–neutral reactions have been considered with the neutral species C_2H_2, H_2, and the radical species C_4H_2, C_6H_2, and C_8H_2. The electron–radical reactions are also considered because it is found that these radical species are abundant at high densities in the discharge (see the following). For the ionization reactions of acetylene, the partial cross sections are only known at higher electron energy (region 100–1000 eV) [16]. Hence, the partial ionization cross sections in the lower electron energy region are obtained by fitting, based on the total ionization cross section (which is known in the whole electron energy region), and starting from the threshold energies for the given ions [16]. For the dissociation reaction of acetylene (into C_2H and H), no cross section was found in literature. As an approximation, an electron excitation cross section was used here. The approach of using electron excitation cross sections for unknown dissociation cross sections has also been applied for the modeling of CH_4 plasmas with reasonable results (i.e., a good agreement was obtained between the calculated and experimental species densities) [1], and it gives also reasonable results for the present simulations (see further). For the carbon rich radicals (C_4H_2, C_6H_2, and C_8H_2), no information concerning cross sections can be found and, hence, approximations have been used in this case as well.

In total, one ion–neutral (Table III) and 17 neutral–neutral reactions (Table IV) are included in the model. The ion–neutral reaction between $C_2H_2^+$ and C_2H_2 is described in detail in [6]. An intermediate ion ($C_4H_4^{+*}$) is assumed, leading to the formation of the ions $C_4H_4^+$, $C_4H_3^+$, $C_4H_2^+$, and $C_2H_3^+$. As an assumption, only the formation of the ion $C_4H_2^+$ is considered in the model (hence also neglecting the intermediate ion state). Since no reaction rate coefficient for this reaction is found in literature, a value of 10^{-15} m^3/s is assumed, based on data for other ion–neutral

TABLE III
ION–NEUTRAL REACTIONS TAKEN INTO ACCOUNT IN THE MODEL

Ion-neutral reactions	Reaction rate coefficient (m^3/s)	Ref.
$C_2H_2 + C_2H_2^+ \rightarrow C_4H_2^+ + H_2$	1.0×10^{-15}	6 *

*: reaction rate coefficient is not known from literature, hence, this value is assumed based on data for similar ion-neutral reactions.

TABLE IV
NEUTRAL–NEUTRAL REACTIONS INCORPORATED IN THE MODEL

Neutral-neutral reactions	Reaction rate coefficient (m^3/s)	Ref.
$C_2H + C_2H_2 \rightarrow C_4H_2 + H$	4.0×10^{-17}	5
$C_2H + C_4H_2 \rightarrow C_6H_2 + H$	5.0×10^{-18}	5 *
$CH + H_2 \rightarrow CH_2 + H$	6.8×10^{-19}	21
$C_2H + H_2 \rightarrow C_2H_2 + H$	1.3×10^{-19}	21
$C_2H + H \rightarrow C_2H_2$	3.0×10^{-16}	22
$CH_2 + H \rightarrow CH + H_2$	2.7×10^{-17}	23
$CH_2 + CH_2 \rightarrow C_2H_2 + H_2$	5.3×10^{-17}	24
$H + C_2H_2 \rightarrow C_2H_3$	1.0×10^{-21}	5
$H + C_4H_2 \rightarrow C_4H_3$	2.6×10^{-18}	5
$H + C_6H_2 \rightarrow C_6H_3$	2.6×10^{-18}	5 *
$H + C_2H_3 \rightarrow C_2H_2 + H_2$	2.0×10^{-17}	21
$C_2H + C_2H_3 \rightarrow C_2H_2 + C_2H_2$	1.6×10^{-18}	22
$H + C_4H_3 \rightarrow H_2 + C_4H_2$	2.0×10^{-17}	5
$H + C_6H_3 \rightarrow H_2 + C_6H_2$	2.0×10^{-17}	5 *
$C_4H + C_2H_2 \rightarrow C_6H_2 + H$	5.0×10^{-18}	5 *
$C_2H + C_6H_2 \rightarrow C_8H_2 + H$	5.0×10^{-19}	5 *
$C_6H + C_2H_2 \rightarrow C_8H_2 + H$	5.0×10^{-19}	5 *

*: reaction rate coefficients are estimated.

reactions [1]. It will be shown later that this fitting value yields good agreement between the calculated species densities from the model and the experimental data available in literature. The neutral–neutral reactions are obtained from different sources, and are presented in Table IV. Some reaction rate coefficients which are not known from literature, are fitted. The use of fitting parameters is a common approach in modeling when exact data are lacking [1], [5], [25]. Finally, it should also be noticed that nearly no information is available on electron–neutral or neutral–neutral reactions, in which the higher carbon molecules (like C_4H_2, C_6H_2, and C_8H_2) dissociate in two (or more) carbon rich species, by breaking a carbon–carbon bond. A possible reason is that the carbon–carbon bonds in these molecules have a strong double or triple bond character, which makes it quite difficult to break them. Hence, it is more likely that if a reaction occurs, a carbon-hydrogen bond will be broken (for example: $e^- + C_4H_2 \rightarrow C_4H + H + e^-$). Only for C_2H_2, three electron-C_2H_2 reactions (i.e., dissociative ionization reactions) are described in literature in which the carbon–carbon bond is broken (see Table II). However, the cross sections of these electron-neutral reactions are rather low, and they are all characterized by a rather high threshold energy (i.e., about 20 eV).

In order to predict the layer growth, a deposition model is included by means of "sticking coefficients." For the radicals C_2H_3, C_4H_3, and C_6H_3, a sticking coefficient of 0.3 is used [26], whereas this is 0.25 for the species CH and CH_2 [1]. It is known from literature [26] that the C_2H species have a large sticking coefficient (i.e., in the order of 0.8). However, it should be mentioned that a somewhat lower value is obtained from other studies [24], [27]. Since this sticking coefficient is subject to a large uncertainty, we have slightly adapted this value, in order to match the theoretical deposition rate with the experimental values obtained by Doyle [28] (in the power region of 0–20 W, giving deposition rates in the order of 0.05–0.4 nm/s). As an approximation, the radicals C_4H_2, C_6H_2, and C_8H_2, present in the discharge at high densities, are not considered in the deposition model (i.e., the sticking coefficients of these species are set to zero). Note that, for similar plasma conditions, the deposition rates obtained using an acetylene plasma [5], are higher compared to a methane plasma [4].

III. RESULTS OF THE MODEL

In this section, the results of several simulations will be discussed and compared with other (experimental and theoretical) data available from literature. The reactor radius of the plasma reactor is set to 10 cm, while the distance between the two electrodes is 3 cm. In Section III-A, the results of the acetylene plasma will be discussed. In Section III-B, a comparison is made between the results of an acetylene and a methane [1] plasma.

A. C_2H_2 *Discharge*

For the simulations of the acetylene plasma, an input gas flow of 20 sccm acetylene is used. The power going into the plasma is 10 W, while the pressure is set to 0.14 torr.

In Fig. 1, the densities of the most important species (neutrals, radicals, ions, and electrons) are given, as a function of distance between the electrodes (3 cm). As can be seen from this figure, the most important nonreactive neutrals are C_2H_2 and H_2. Despite of the fact that no H_2 molecules are introduced in the plasma, the hydrogen density is very high. This can be explained from the ion–neutral (Table III) and neutral–neutral reactions (Table IV), in which a lot of H_2 molecules are formed. Similar results were also obtained for the modeling of methane [1] and silane [13]–[15] plasmas. Further, the radicals C_4H_2, C_6H_2, and C_8H_2 are also present at high densities. These species are mainly formed in the neutral–neutral reactions with C_2H. The presence of these species at high densities in an acetylene plasma is also found by others [5], [6].

Other radicals present in the discharge at relative high densities are H, C_2H, and C_xH_3 (with $x = 2, 4$, and 6). In Fig. 1, only

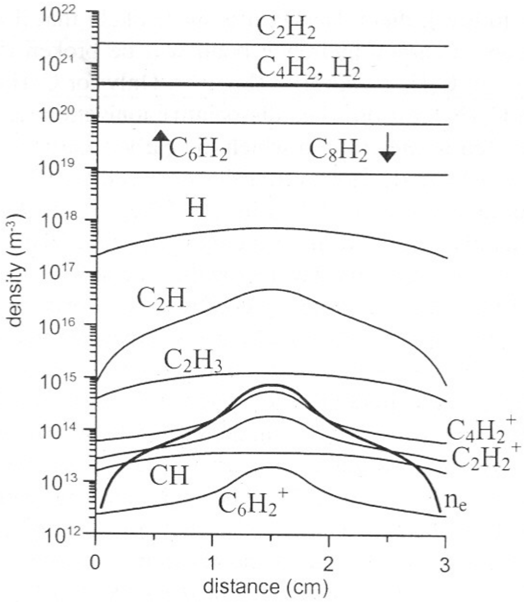

Fig. 1. Calculated densities (m^{-3}) of the nonradical neutrals, radicals, ions, and electrons as a function of distance from the electrode at 0.14 torr, 10 W, 13.56 MHz, and 20 sccm acetylene inlet.

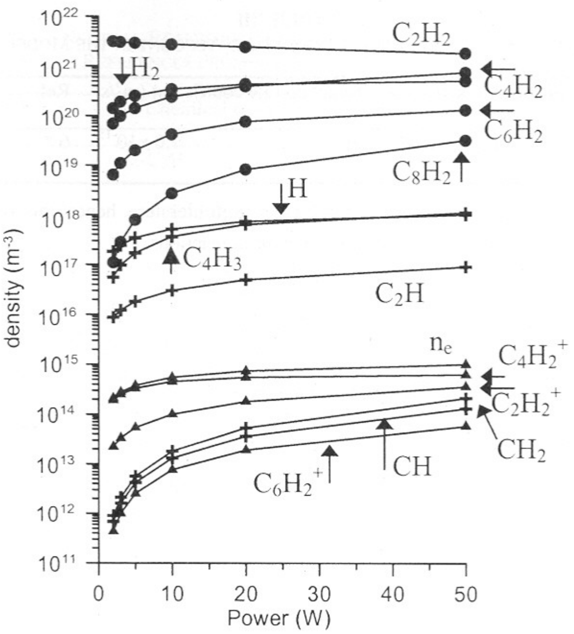

Fig. 2. Calculated densities (m^3) of the nonradical neutrals, radicals, ions, and electrons as a function of generator plasma (acetylene). The other parameters are kept the same as in Fig. 1.

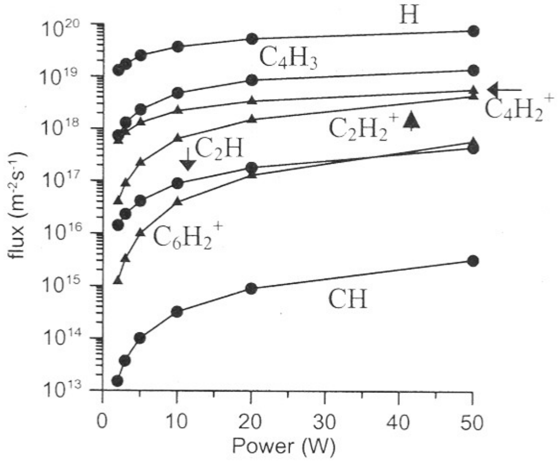

Fig. 3. Calculated radical and ion fluxes $(m^{-2}s^{-1})$ toward the electrodes as a function of generator power (acetylene plasma). The other parameters are kept the same as in Fig. 1.

the density of C_2H_3 is presented. The densities of C_4H_3 and C_6H_3 (not shown in Fig. 1) are in the order of 10^{16} m^{-3}. Further, it can also be seen that the species C_xH (with $x = 2, 4, 6,$ and 8) are present in the discharge at rather high densities. Since all C_xH species have comparable densities, only the density of C_2H is presented on Fig. 1. Unfortunately, no experimental data on the densities of these species are available in literature, and hence, no comparison with the calculated data we obtained, was possible. At last, the densities of CH_2 and CH are in the order of $10^{13}m^3$ (only the density of CH is given in Fig. 1).

The most important ionic species are found to be $C_4H_2^+$, $C_2H_2^+$, and $C_6H_2^+$, respectively. These results were also obtained from experiments [6], [29]. Finally, the electron density is also given in Fig. 1. Since the electron density shows considerable variations in the sheath zones, during the rf cyclus, the time-averaged electron density is given. Although the ion densities do hardly vary during the RF cycle, also the time-averaged ion density profiles are given in Fig. 1. Results of a mass spectrometry study of the acetylene plasma by Deschenaux *et al.* [29] show the presence of the species with mass 2 (H_2), 13 (CH), 25 (C_2H), 27 (C_2H_3), 49 (C_4H), 50 (C_4H_2), and 51 (C_4H_3), which are also considered in our model.

In Fig. 2, the densities of various plasma species are plotted as a function of power. It is worth mentioning that we assumed that the input power (i.e., the power going into the plasma) is half of the generator power [1], [13]. The x axis in Fig. 2 is the generator power. As can be seen from this figure, the density of C_2H_2 decreases as a function of power, which is logical because the higher the power, the more C_2H_2 is "consumed" in the different reactions. All other densities increase as a function of power, because they are formed in the chemical reactions.

In Fig. 3, the fluxes $(m^{-2} \cdot s^{-1})$ of the different species toward the electrodes are given, as a function of power. As can be seen from this figure, all species fluxes increase significantly at low power, and more slightly at high power. The fluxes of the radical species C_xH are all of the same order, hence only the C_2H flux is given. The same conclusions can be drawn for the fluxes of the species C_xH_3, for which only C_4H_3 is given. Note that, due to the limitations of the 1-D model, the fluxes toward both electrodes (i.e., powered and grounded electrode) are equal.

B. Comparison of the Results Obtained for an Acetylene and a Methane Plasma

In order to compare the results of a methane plasma with an acetylene plasma, a number of simulations (13.56 MHz, 0.14 torr) were obtained for a methane plasma (described in detail in [1]), with varying power (Fig. 4). It can be seen that, when comparing Fig. 4 (methane plasma) and Fig. 2 (acetylene plasma), both plasmas are characterized by a number of neutral background gases, present at high densities in the discharge,

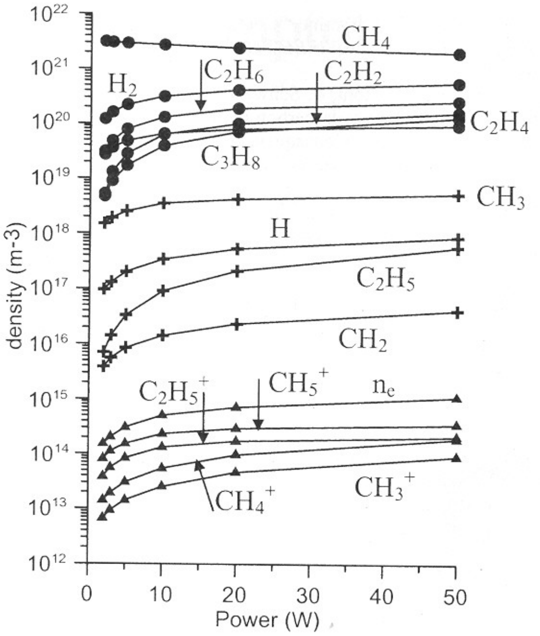

Fig. 4. Calculated densities (m^3) of the nonradical neutrals, radicals, ions, and electrons as a function of generator plasma (methane). The other parameters are kept the same as in Fig. 1.

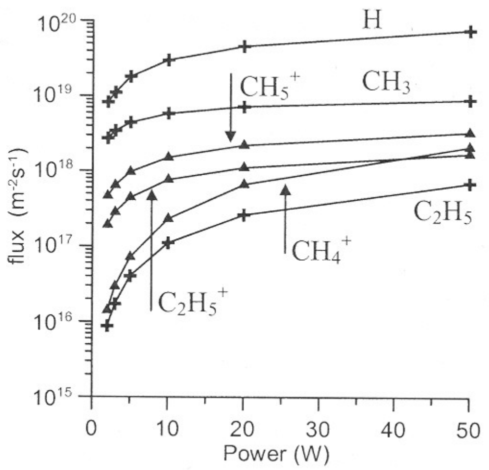

Fig. 5. Calculated radical and ion fluxes $(\mathrm{m}^{-2}\cdot\mathrm{s}^{-1})$ toward the electrodes as a function of generator power (methane plasma). The other parameters are kept the same as in Fig. 1.

and formed in the neutral–neutral chemistry. Typical for an acetylene discharge is the presence of the radical species C_4H_2, C_6H_2, and C_8H_2 at high densities. These species are formed in the neutral–neutral reactions with C_2H (see Table IV). In a methane plasma, the neutral species C_2H_2, C_2H_4, C_2H_6, and C_3H_8 are abundant at relatively high densities, while the most important radicals are found to be CH_3, H, and C_2H_5. Beside the radical species C_xH_y $(x > y)$ mentioned previously, the radicals H, C_2H, and C_xH_2 (with x equal to 2, 4, and 6) are also present in the acetylene discharge. The fact that other radical species $(C_2H, C_xH_2, \ldots)$ are present in an acetylene discharge, compared to a methane plasma [1], can be explained from the neutral–neutral chemistry, which is totally different in both plasmas. The neutral–neutral chemistry in an acetylene discharge depends strongly on the reactions of C_2H with other species (see Table IV), while the neutral–neutral chemistry in a methane plasma is characterized by reactions between all kinds of species $(CH_4, CH_3, CH_2, H, C_2H_5, \ldots)$. It is also worth mentioning that, whereas in the methane plasma model seven ion–neutral reactions were considered [1], only one ion–neutral reaction is found to be important in the acetylene plasma (Table III). The most important ions in a methane plasma are CH_5^+, $C_2H_5^+$ (formed in the ion–neutral chemistry), and CH_4^+ and CH_3^+, created in the electron–methane ionization reactions. In an acetylene plasma on the other hand, the species $C_4H_2^+$, $C_2H_2^+$, and $C_6H_2^+$ are found to be the most prevalent ionic species.

When comparing the species fluxes to the electrodes in an acetylene (Fig. 3) and a methane plasma (Fig. 5), it can be seen that the H radical flux is comparable in both cases. Further, the fluxes of the species C_xH_3, C_xH, and $C_xH_2^+$ (with x equal to 2, 4, and 6) are important in an acetylene plasma, whereas the methane plasma yields the species fluxes of CH_3, C_2H_5, CH_5^+, and $C_2H_5^+$ toward the electrodes. Hence, it can be concluded that both plasmas are characterized by other species fluxes toward the substrates, influencing the growth of the amorphous carbon layer. It is found that, when using an acetylene plasma, higher deposition rates are obtained [5], compared to a methane plasma [4]. However, a detailed investigation of these plasma-wall interactions is beyond the scope of this paper.

IV. CONCLUSION

A 1-D fluid model is presented for the modeling of acetylene RF discharges. In the model, 24 species are considered. Beside the neutral species (C_2H_2 and H_2) and the electrons, a number of ions (8) and radicals (13) are included. Consequently, a large number of chemical reactions are taken into account in the model. Assumptions are made for some reaction rate coefficients of the ion–neutral and neutral–neutral reactions, and for some cross sections, needed to calculate the reaction rate coefficient for the different electron–neutral reactions.

It is found that the neutral species C_2H_2 and H_2 are present in the discharge at high density, together with a number of hydrocarbon molecules (C_4H_2, C_6H_2, and C_8H_2). The other radical species are also present in the discharge at relatively high densities, because they are formed in the neutral–neutral reactions. The main ions in the model are $C_2H_2^+$, $C_4H_2^+$, and $C_6H_2^+$. A number of $C_2H_2^+$ ions react further (in an ion–neutral reaction with C_2H_2) to form $C_4H_2^+$. Further, a comparison is made between a methane and an acetylene plasma, both used for the deposition of amorphous carbon layers. It is found that both discharge gases yield a completely different chemistry. Finally, a simple deposition model is—as a first approximation—included. However, it is worth mentioning that we are currently working on a far more detailed deposition model by means of a molecular deposition model, in order to get a better description of the growth of the layer.

ACKNOWLEDGMENT

The authors wish to thank A. Phelps for his useful information about the cross sections used in this model and J. Doyle for supplying interesting experimental data concerning the deposition rates in an acetylene plasma.

REFERENCES

[1] D. Herrebout, A. Bogaerts, M. Yan, R. Gijbels, W. Goedheer, and E. Dekempeneer, "One dimensional fluid model for an RF methane plasma of interest in deposition of diamond-like carbon layers," *J. Appl. Phys.*, vol. 90, pp. 570–579, 2001.

[2] E. Gogolides, D. Mary, A. Rhaballi, and G. Turban, "RF plasmas in methane: Prediction of plasma properties and neutral radical densities with combined gas-phase and chemistry model," *Jpn. J. Appl. Phys.*, vol. 34, pp. 261–270, 1995.

[3] E. Gogolides, C. Buteau, A. Rhallabi, and G. Turban, "Radio frequency glow discharges in methane gas modeling of the gas phase physics and chemistry," *J. Phys. D, Appl. Phys.*, vol. 27, pp. 818–825, 1994.

[4] E. Dekempeneer, J. Smeets, J. Meneve, L. Eersels, and R. Jacobs, "Plasma processes in methane discharges during RF plasma-assisted chemical vapor deposition of a-C:H thin films," *Thin Solid Films*, vol. 241, pp. 269–273, 1994.

[5] R. Doyle, "Chemical kinetics in low pressure acetylene radio frequency glow discharges," *J. Appl. Phys*, vol. 82, p. 4763, 1997.

[6] M. J. Vasile and G. Smolinsky, "The chemistry of radio frequency discharges: Acetylene and mixtures of acetylene with Helium, Argon and Xenon," *Int. J. Mass. Spectrom. Ion. Phys.*, vol. 24, pp. 11–23, 1977.

[7] I. Platzner and P. Marcus, "Condensation reactions in a microwave-induced acetylene plasma," *Int. J. Mass Spectrom. Ion Phys.*, vol. 41, pp. 241–250, 1982.

[8] K. H. Lai, C. Y. Chan, M. K. Fung, I. Bello, C. S. Lee, and S. T. Lee, "Mechanical properties of dlc films prepared in methane plasmas using electron cyclotron resonance microwave plasma chemical deposition," *Diamond Rel. Mater.*, vol. 10, p. 1862, 2001.

[9] A. De Graaf, M. F. A. M. Van Hest, M. C. M. van de Sanden, K. G. Y. Letourneur, and D. C. Schram, "Argon ion-induced dissociation of acetylene in an expanding $\mathrm{Ar}/\mathrm{C_2H_2}$ plasma," *Appl. Phys. Lett.*, vol. 74, p. 2927, 1999.

[10] A. D. Graaf, G. Dinescu, J. L. Longueville, M. C. M. van de Sanden, D. C. Schram, E. H. A. Dekempeneer, and L. J. van Ijzendoorn, "Amorphous hydrogenated carbon nitride films deposited via an expanding thermal plasma at high growth rates," *Thin Solid Films*, vol. 333, pp. 29–34, 1998.

[11] J. W. A. M. Gielen, W. M. M. Kessels, M. C. M. van de Sanden, and D. C. Schram, "Effect of substrate conditions on the plasma beam deposition of amorphous hydrogenated carbon," *J. Appl. Phys.*, vol. 82, p. 2643, 1997.

[12] J. W. A. M. Gielen, M. C. M. van de Sanden, and D. C. Schram, "Plasma beam deposited amorphous hydrogenated carbon: Improved film quality at high growth rate," *Appl. Phys. Lett.*, vol. 69, pp. 152–154, 1996.

[13] G. J. Nienhuis, W. J. Goedheer, E. A. G. Hamers, W. G. J. H. M. van Sark, and J. Bezemer, "A self-consistent fluid model for radio-frequency discharges in $\mathrm{SiH_4}/\mathrm{H_2}$ compared to experiments," *J. Appl. Phys.*, vol. 82, pp. 2060–2071, 1997.

[14] G. J. Nienhuis and W. J. Goedheer, "Modeling of a large scale reactor for plasma deposition of silicon," *Plasma Sources Sci. Technol.*, vol. 8, pp. 295–298, 1999.

[15] G. J. Nienhuis, "Plasma models for silicon deposition," Ph.D. dissertation, Dept. Phys., Univ. Utrecht, Utrecht, The Netherlands, 1998.

[16] H. Tawara, Y. Itikawa, H. Nishimura, H. Tanaka, and H. Nakamura, *Collision data involving hydro-carbon molecules*. Nagano, Japan: NIFS-DATA-6, 1990.

[17] H. Tawara, *Electron Collision Processes Involving Hydrocarbons Atomic and Molecular Processes in Fusion Edge Plasmas*, R. K. Janev, Ed. New York: Plenum, 1995, pp. 461–495.

[18] L. Ehrhardt, L. Langhans, F. Linder, and H. S. Taylor, "Resonance scattering of slow electrons from hydrogen and CO angular distributions," *Phys. Rev*, vol. 173, pp. 222–230, 1968.

[19] A. G. Engelhardt and A. V. Phelps, "Elastic and inelastic collision cross sections in hydrogen and deuterium from transport coefficients," *Phys. Rev*, vol. 131, pp. 2115–2128, 1963.

[20] H. Tawara and T. Kato, *At. Data Nucl. Data Tables*, 1987, vol. 36, pp. 167–353.

[21] D. L. Baulch *et al.*, "Evaluated kinetic data for combustion modeling," *Phys. Chem. Ref. Data*, vol. 21, pp. 411–734, 1992.

[22] W. Tsang and R. F. Hampson, "Chemical kinetic data base for combustion chemistry. Part 1: Methane and related compounds," *J. Phys. Chem. Ref. Data*, vol. 15, pp. 1087–1279, 1986.

[23] L. E. Kline, W. D. Partlow, and W. E. Bies, "Electron and chemical kinetics in methane RF glow discharge deposition plasmas," *J. Appl. Phys*, vol. 65, pp. 70–78, 1988.

[24] A. De Graaf, "Deposition of CNH materials: Plasma and film characterization," Ph.D. dissertation, Dept. Phys., Univ. Eindhoven, Eindhoven, The Netherlands, 2000.

[25] A. Rhallabi and Y. Catherine, "Computer simulation of a carbon deposition plasma in methane," *IEEE Trans. Plasma Sci.*, vol. 19, pp. 270–277, Apr. 1991.

[26] A. V. Keudell, C. Hopf, T. Schwarz-Selinger, and W. Jacob, "Surface loss probabilities of hydrocarbon radicals on amorphous hydrogenated carbon film surfaces: Consequences for the formation of re-deposited layers in fusion experiments," *Nucl. Fusion*, vol. 39, pp. 1451–1462, 1999.

[27] M. D. Perry and L. M. Raff, "Theoretical study of elementary chemisorption reactions on activated diamond (111) terrace," *J. Phys. Chem.*, vol. 98, p. 8128, 1994.

[28] R. Doyle, private communication.

[29] C. Deschenaux, A. Affolter, D. Magni, and C. H. P. Fayet, "Investigation of $\mathrm{CH_4}$, $\mathrm{C_2H_2}$ and $\mathrm{C_2H_4}$ dusty RF plasmas by means of FTIR absorption spectroscopy ad mass spectroscopie," *J. Phys. D, Appl. Phys.*, vol. 32, p. 1876, 1999.

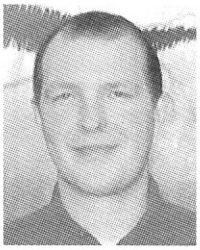

Dieter Herrebout is working toward the Ph.D. degree at the University of Antwerp, Wilrijik, Belgium, where his research focuses on the modeling of the plasma chemistry of methane and acetylene plasmas

Annemie Bogaerts was born in 1971. She received the M.Sc. degree in chemistry and the Ph.D. degree in sciences from the University of Antwerp, Wilrijik, Belgium, in 1993 and 1996, respectively.

She is currently a Postdoctoral Researcher at the University of Antwerp, but will become a Professor of physical chemistry on October 1, 2003. Her research interests include the modeling of glow discharges and related plasmas, plasma solids, ion solids, and laser solid interaction.

Renaat Gijbels has been a Professor of physical chemistry at the University of Antwerp, Wilrijik, Belgium, since 1973. His research interests include various types of inorganic mass spectrometry for bulk, surface and/or microanalysis, e.g., spark, laser ionization, and secondary ion and glow discharge mass spectrometry.

Willem Jan Goedheer was born in The Netherlands in 1950. He received the physics and Ph.D. degrees from the University of Utrecht, Utrecht, The Netherlands, in 1973 and 1978, respectively.

Since 1973, he has been with the FOM-Institute for Plasma Physics, Nieuwegein, The Netherlands, where he has been mainly involved in modeling of partially ionized plasma, both in the boundary layers of a Tokamak and in industrial applications, including dusty and colloidal plasmas in capacitively coupled RF discharges.

Annick Vanhulsel received the engineering degree in materials science and the Ph.D. degree in applied science from the University of Leuven, Leuven, Belgium.

She is currently a Staff Member of the Plasma Technology Group, Vlaamse Instelling voor Technologisch Onderzoek, Belgium. Her primary research interests include the development and study of plasma deposited functional coatings, such as antisticking, hydrophobic, low-friction coatings. She has been working on several national and international projects in the field of plasma technology and coating development.